Wind-Tunnel Tests of a Bridge Model with Active Vibration Control

Hansen, H. I.; Thoft-Christensen, Palle; Mendes, P. A.; Branco, F. A.

Publication date:
2000

Document Version
Publisher's PDF, also known as Version of record

Aalborg **UNIVERSITY**

Wind-Tun

Wind-Tunnel Tests of a Bridge Model with Active Vibration Control

H.I. Hansen, P. Thoft-Christensen,
P.A. Mendes, F.A. Branco

Paper No 198

Structural Reliability Theory

In: Structural Engineering International, Vol. 10. No. 4,
2000, pp. 249-253.

ISSN 1395-7953 R0019

Printed at Aalborg University

Wind-Tunnel Tests of a Bridge Model with Active Vibration Control

H.I. Hansen, P. Thoft-Christensen,
P.A. Mendes, F.A. Branco

WIND -TUNNEL TESTS OF A BRIDGE MODEL WITH ACTIVE VIBRATION CONTROL

H. I. Hansen	P. Thoft-Christensen	P. A. Mendes	F. A. Branco
Ph.D.	Prof. Civil Eng.	Assoc. Prof.	Prof. Civil Eng.
Univ. Aalborg	Univ. Aalborg	IST - Lisbon	IST - Lisbon

Summary

The application of active control systems to reduce wind vibrations in bridges is a new area of research. This paper presents the results that were obtained on a set of wind tunnel tests of a bridge model equipped with active movable flaps. Based on the monitored position and motion of the deck, the flaps are regulated by a control algorithm so that the wind forces exerted on them counteract the deck oscillations.

Introduction

The tendency to increase the span length of cable-stayed and suspension bridges has increased the importance of wind effects on such structures, and aerodynamic issues are often crucial to the design. The accidents that have occurred on bridges due to wind led to a significant amount of research in this area and, nowadays the design of important bridges involves both numerical model-based and wind tunnel studies to achieve structural solutions that are not, or only slightly wind-sensitive.

In addition to the problems that may arise from aerodynamic instability, several bridges also present large-amplitude vibrations even under moderate wind speeds, which lead to the frequent closing of the bridge to traffic and the associated social and economic inconvenience.

In order to solve mainly this second type of problem, a new strategy is being investigated by the scientific community [1,2]. This strategy consists of the installation of active control systems that are activated under wind vibration situations, in order to reduce vibration levels and guarantee the serviceability conditions of the structure.

This paper presents the results from a series of wind tunnel tests that were performed for a bridge model equipped with active movable flaps [3]. The idea for this control system [4, 5] (Fig. 1) based on damping the oscillations of the deck through the forces exerted on the flaps by the wind. Based on the monitored position and motion of the deck, the flaps are regulated by a control algorithm so that the wind forces exerted on them counteract the deck oscillations.

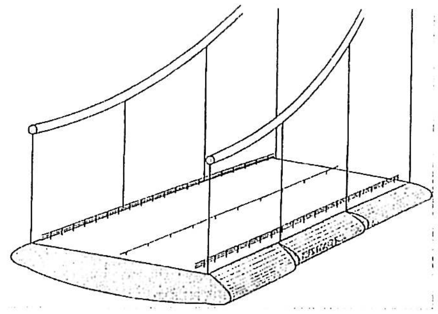

Fig.1: Flaps on a bridge girder

In real bridges these flaps will be divided into segments along the span. Each segment may then be regulated independently and it is expected that these flaps will not need to be mounted over the entire span of the bridge.

Wind-Tunnel Tests

The tests were performed in a wind tunnel of the open return type. A contraction unit 3.00 m long (with a length:width ratio of 5.44:1) takes the air to the test chamber, which has a cross section 1.50 m x 1.50 m (at the entrance) and is 5.00 m long. After the test chamber, there is a diffuser allowing the transition from the square shape to a circular duct, 1.80 m in diameter, where the fan is located.

The fan is of the variable-pitch type and works at a constant speed of rotation (1470 rpm). The pitch is controlled manually by a compressed-air system. The maximum wind speed inside the test section is 40m/s. The wind speed is measured by using a Pitot-Prandtl tube connected to a pressure transducer.

Bridge Model

Figure 2 illustrates the cross section of the model that was tested. The width of the model, excluding the flaps, is denoted by B' and the height of the model is $0.15B'$. The width of each flap is $0.25B'$, so that the total width (B) is equal to $1.50B'$.

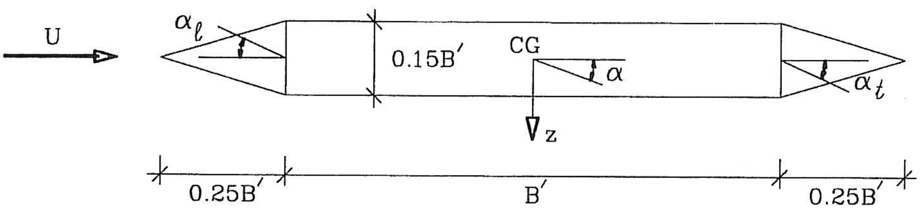

Fig.2: Cross section of the model (B' = 62 5mm)

The model was made as light as possible, because the part of the regulation system to be fixed inside the model (namely two servomotors and two reduction gears) is relatively heavy. Thus, the model was made of foam with an aluminium frame to make it stiff. This frame was provided with holes, where possible, in order to reduce its weight. The space between the model and the flaps was closed by a piece of fabric in order to prevent the flow from being separated in this region (Fig.3).

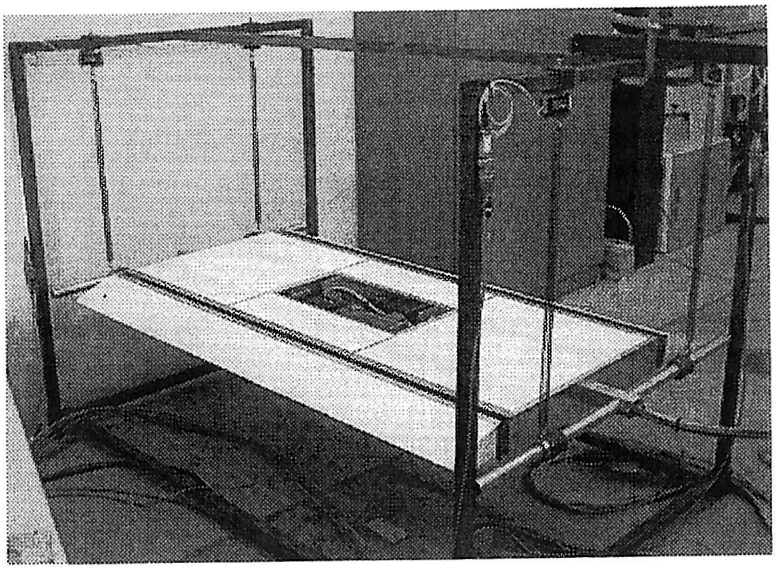

Fig. 3: View of the model

The model was 1480 mm long and was connected on each side to a horizontal extension rod. Each rod was connected to an arm with dummy masses in order to represent the correct mass and mass inertia. The arms were suspended on each side by helical springs that could be moved along the arm in order to adjust the torsional frequency.

During the experiments, the motion of the model was measured by four load cells. The movements in the wind direction were prevented by using long drag wires attached to the steel frames. Figure 4 illustrates the model in the wind tunnel.

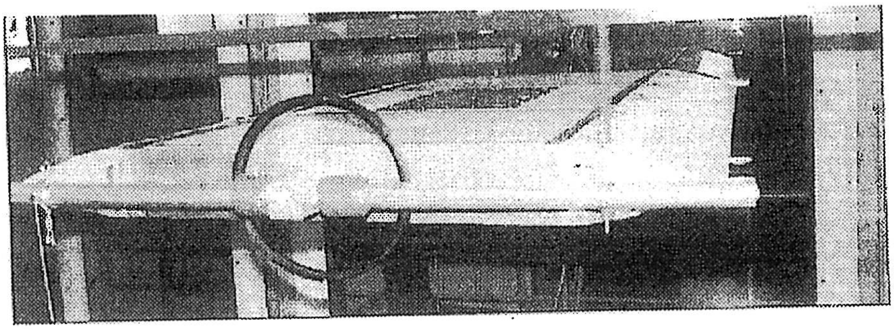

Fig. 4: Testing in the wind tunnel

The scales adopted for the experiments were: λ_L = 1:40 (length), λ_V = 1:4 (velocity) and λ_ρ = 1 (mass density). Based on these fundamental values, the frequency scale was $\lambda_f = \lambda_V / \lambda_L$ = 10:1 and the mass-per-unit-length scale is $\lambda_\mu = \lambda_\rho (\lambda_L)^2$ = 1:1600. The values assumed for the prototype and the corresponding values for the model are shown in Table1.

Characteristic		Prototype (assumed)	Model (theoretical)
Width of the deck (B')	(m)	25	0.625
Total width (B)	(m)	37.5	0.9375
Mass per unit length (with no flaps)	(kg/m)	25 000	15.625
Mass per unit length of each flap	(kg/m)	1160	0.725
Mass moment of inertia per unit length	(kg.m²/m)	2.1x10⁶	0.820
First eigenfrequency (bending)	(Hz)	0.08	0.80
Second eigenfrequency (torsion)	(Hz)	0.16	1.60

Table 1: Characteristics assumed for the prototype and corresponding model values

The critical wind speed for coupled flutter in a flat plate (U_{cr}) may be estimated by the Selberg's formula:

$$\frac{U_{cr}}{f\alpha^{B}} = 3.72\sqrt{\frac{\sqrt{I\mu}}{\rho B^{3}}\left(1-\left(\frac{f_z}{f_\alpha}\right)^{2}\right)} \tag{1}$$

where μ and I are the mass properties per unit length, f_z and f_α are the frequencies of oscillation and ρ is the volumic mass of the air.

The values assumed for the prototype and for the velocity scale were chosen in order to get a flutter wind speed around 10 m/s, which is a value easily attainable in the wind tunnel. If the values assumed for the prototype are taken, namely B = 37.5 m, I = 2.1 x 10^6 kg.m²/m, μ = 27320 kg/m, f_z = 0.08 Hz and f_α = 0.16 Hz, and ρ = 1.28 kg/m³, then U_{cr} = 36.4 m/s. Thus, with λ_V = 1:4, the expected flutter wind speed in the tunnel is U_{cr} = 9.1 m/s.

Considering the length of the model (1.48 m) and the values shown in Table 1, the theoretical value of the total oscillating mass is M = 25.271 kg. Thus, in order to get the desired frequency for the vertical motion (f_v = 0.80 Hz), the four helical springs were ordered with a stiffness k given by:

$$f_v = \frac{1}{2\pi}\sqrt{\frac{4k}{M}} \Leftrightarrow k = \frac{N(M\pi f_v)^2}{4} = 160 \text{ N/m} \tag{2}$$

Flap Regulation System

The regulation system to move the flaps consists of two servo systems, the regulation software to position the flaps and the control software to calculate the desired position of the flaps.

Each servo system consists of a servo amplifier, a servomotor and a reduction gear. Two servo systems are used as the flaps are regulated independently. The servo amplifiers are placed outside the model, while the servomotors and the reduction gears are fixed inside the model. Each reduction gear is connected to a flap via cables. Regarding the regulation software, the position regulator is basically a proportional integral derivative (PID) regulator in the servo amplifier.

During the experiments the flaps can only be regulated by the software, i.e., there is no manual control. If the flaps turn too much, with risk of damaging the model, the motors may be cut off by switches in the model.

Calibration of the Model

The total mass of the model after construction, including flaps, was measured as 26.553 kg (i.e., μ = 17.94 kg/m). This value is only 5% above the theoretical one (25.271 kg) and so the consequences of this difference were disregarded. With respect to the eigenfrequencies, the mean value for the vertical motion was 0.83 Hz (versus a desired value of 0.80 Hz) and for the torsional motion the value 1.61 Hz was obtained (versus 1.60 Hz) with the distance between the springs ($2a$) being 704 mm.

Based on these results, the global stiffness of the model in bending and in torsion (denoted by k_z and k_α, respectively) and its equivalent mass moment of inertia (I) per unit length were estimated through the following expressions:

$$k_z = (2\pi f_z)^2 \mu = 488 \text{ N/m}^2 \tag{3}$$

$$k_\alpha = a^2 k_z = 60.5 \text{ N} \tag{4}$$

$$I = \frac{k_\alpha}{(2\pi f_\alpha)^2} = 0.590 \text{ kg.m}^2\text{/m} \tag{5}$$

The values measured for the structural damping ratio in bending (ζ_z) and in torsion (ζ_α) were 1.2% and 0.8%, respectively.

If the theoretical flutter derivatives of a flat plate are considered along with this set of experimental values, the corresponding coupled flutter wind speed U_{cr} is 8.18 m/s. Although Selberg's formula does not take into account the real values of damping, it usually provides a good estimate of U_{cr} if f_α/f_z >1.50. In this case, Selberg's formula leads to U_{cr} = 8.5 m/s. This order of magnitude of the critical wind speed was in fact observed in the wind tunnel in the case of fixed flaps (configuration 0).

Experimental Results

The main purpose of the first set of wind tunnel experiments was to investigate how the effective damping of the model depends on the flap configuration for variable wind velocities. Thus, for simplicity, the initial tests were performed with the two flaps moving with the same phase angle, which is not an optimal solution. With this simple control algorithm, the desired angles of the trailing and leading flaps α_t and α_l, respectively are given by:

$$\alpha_t(t) = a_t\,\alpha(t) \tag{6}$$

$$\alpha_l(t) = a_l\,\alpha(t) \tag{7}$$

where a_t and a_l are amplitude amplification factors and $\alpha(t)$ is the torsional angle exhibited by the model at time t. The following configurations were tested:

- configuration 0:	$a_t = a_l = 0$;	
- configuration 1:	$a_t = -6$;	$a_l = 6$;
- configuration 2:	$a_t = -20$;	$a_l = 20$;
- configuration 3:	$a_t = 6$;	$a_l = -6$;
- configuration 4:	$a_t = 20$;	$a_l = -20$.

For each configuration both the vertical and the torsional motions were recorded within a range of wind speeds. All the experiments were repeated 3-5 times. The flaps were started slowly by multiplying the desired positions by a factor t/t_0, when $t < t_0$. The value $t_0 = 1$s was considered.

During a damping experiment the following parameters were stored every 12 ms:

- the displacements of the model (vertical z and torsional α);
- the specified angle of the trailing and leading flap (α_t and α_l);
- the actual angle of the trailing and leading flap (α_{ta} and α_{la}).

Fig. 5a-c illustrates the torsional motion for a wind speed of 6.1 m/s and for the flap configurations 0, 2 and 4, respectively. The results show that the global damping of the oscillations can be rather increased (configuration 2); while it is possible to make the flap configuration very unfavourable (e.g. in configuration 4) so that flutter occurs at a lower wind speed than with no flaps moving. The t-axis scale in Fig. 5b is different from the scale in Fig. 5a and 5c because the torsional oscillations in configuration 2 decayed rapidly to zero (as a result of a very high effective damping).

The measurements were noisy and therefore they were filtered, in order to estimate the circular frequency and damping ratio. A second-order filter was used to filter the noisy position measurements after the experiments. This filter is defined by:

$$u_f(k) = 2pu_f(k-1) - p^2u_f(k-2) + (1-p)^2u(k) \tag{8}$$

where $u(k)$ is the noisy measurement at time step k, $u_f(k)$ is the filtered value, and p is the pole. If $p = 0$, the filtered values are equal to the measured values. If $p = 1$, the filtered values do not depend on the measured values. A value of $p = 0.5$ was selected for all the experiments. Fig. 6 illustrates the measured torsional motion and the corresponding filtered motion for flap configuration 2 and $U = 6.1$ m/s.

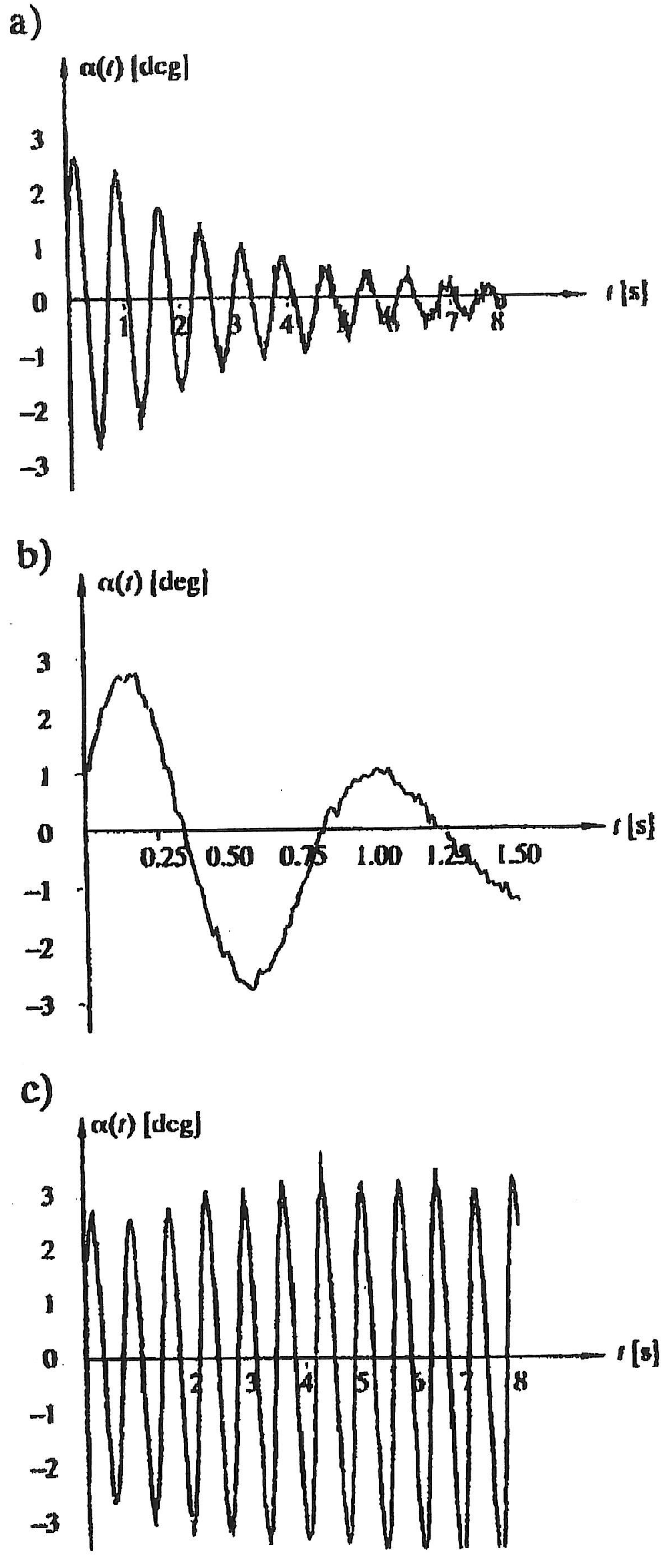

Fig. 5: Torsional motion for different flap configurations (U = 6.1 m/s)

The damping ratio for torsional motion was estimated from the experiments by Hilbert transformation of the filtered time series (Fig. 7). When flap configurations 1 and 2 are used the global damping ratio is increased, whereas when flap configurations 3 and 4 are used the global damping ratio is decreased. The effectiveness of the flaps could not be shown for wind speeds above the critical one.

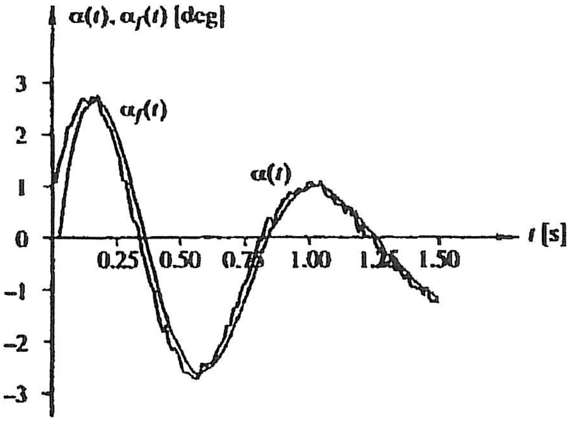

Fig. 6: Measured and filtered torsional motion for flap configuration 2 (U = 6.1 m/s).

Experimental versus Theoretical Results

It is common practice to accept that the motion-induced wind loads on the cross section of a bridge deck depend linearly on the displacements of the deck and on their first time derivatives. This hypothesis comes from the pioneering work of Theodorsen on the behaviour of thin airfoils in incompressible flow.

In the field of bridge aerodynamics, assuming that both the vertical displacements (z) and the rotations (α) of the deck are harmonic (with circular frequency ω), it is usual to work with Eqs. (9) and (10), where L_a and M_a are the motion-induced lift and torsional moment, $K = B\omega/U$ is the so-called reduced frequency and the coefficients $H_1^* - H_4^*$ and $A_1^* - A_4^*$ are aerodynamic derivatives

$$L_a = \frac{1}{2}\rho U^2 B\left[KH_1^*(K)\frac{\dot{z}}{U} + KH_2^*(K)\frac{B\dot{\alpha}}{U} + K^2H_3^*(K)\alpha + K^2H_4^*(K)\frac{z}{B}\right] \tag{9}$$

$$M_a = \frac{1}{2}\rho U^2 B\left[KA_1^*(K)\frac{\dot{z}}{U} + KA_2^*(K)\frac{B\dot{\alpha}}{U} + K^2A_3^*(K)\alpha + K^2A_4^*(K)\frac{z}{B}\right] \tag{10}$$

The theoretical expressions for the aerodynamic derivatives of a thin airfoil (with no flaps) are well known [6]. Based on the principles of potential flow theory, work has been extended to the case of a trailing flap on a thin airfoil. Assuming that the rotation of the leading flap has no effect on the circulation, it can be shown that for the case of a thin airfoil with a leading flap and a trailing flap, both oscillating with the same frequency as the flat plate, Eqs. (9) and (10) still apply with a proper redefinition of the flutter derivatives H_2^*, H_3^*, A_2^* and A_3^* [3].

The theoretical and experimental values of the damping ratios and of the circular frequencies for the torsional motion with the flap configurations 0-4 are shown in Figs.7 and 8. The values shown correspond to the averages of the values that were obtained in the experiments performed for each configuration (3-5 repetitions).

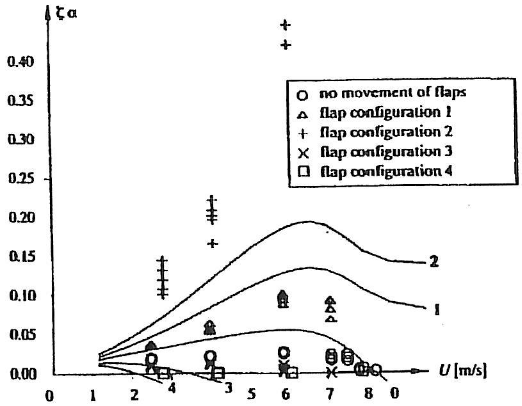

Fig. 7: Theoretical (solid lines) and experimental values of the damping ratio for torsional motion

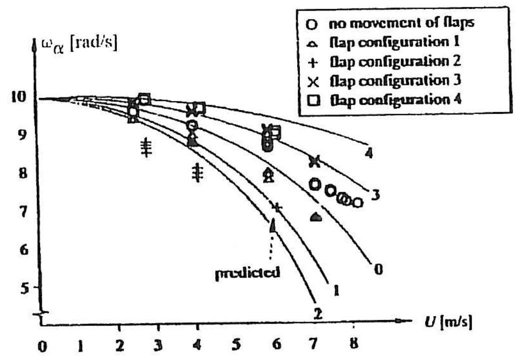

Fig. 8: Theoretical (solid lines) and experimental values of the circular frequency for torsional motion

The estimated frequencies generally follow the theoretical curves for wind velocities below 5 m/s, except for case 2 where the deviations can be caused by the relatively short time series that were recorded (due to the high effective damping). The experimental damping ratio is smaller for cases 0 and 1 than the theoretical damping ratio, but the curve is almost the same. In case 2 the experimental damping is much greater than the theoretical one.

Problems Found during the Experiments

During the preparation of the wind tunnel tests, some unanticipated problems were found, namely:

- noisy measurements of the displacements from the load cells, partly due to the servomotors;
- occurrence of longitudinal (standing) waves in the springs;
- static divergence of the model at a low wind velocity, close to the flutter velocity in configuration 0 (i.e. around 8.5 m/s).

The noisy measurements were dealt with by decreasing the value of P in the PID-regulator, so that the servomotors reacted more slowly and became less sensible to noise.

The occurrence of static divergence limited the range of test velocities in the wind tunnel and was not anticipated in the design of the model, as the attention was focussed on flutter. If a simple two-dimensional approach to the divergence phenomenon on a bridge deck had been considered, the divergence velocity (U_d) would have been estimated through:

$$U_d = \sqrt{\frac{2k_\alpha}{\rho B^2 \frac{dC_M}{d\alpha}}} \tag{11}$$

where C_M is the torsional moment coefficient of the section [6]. Considering that for an ideal flat plate $dC_M/d\alpha = \pi/2$, $k_\alpha = 60.5$ N.m/m, $B = 0.937$ m and $\rho = 1.28$kg/m^3, then $U_d = 8.3$ m/s. This value is similar to the flutter velocity in configuration 0, and such a velocity was observed during the experiments.

Conclusions

A series of wind tunnel tests was performed for a simplified model of a bridge deck equipped with movable flaps regulated actively. Experiments were performed for the model without moving the flaps and with four moving flap configurations, two of them favourable and the other two unfavourable. The phase angle was kept constant during the experiments.

The results obtained clearly show that it is possible to reduce the oscillations and to prevent aerodynamic instabilities by this technique. The damping ratio depends on the wind speed and on the flap configuration, and it may increase considerably even for non-optimal flap configurations. On the other hand, if the movement of the flaps is not regulated properly, then the oscillations may increase as well, with the occurrence of flutter at rather low wind speeds.

The damping and frequency parameters estimated from the wind-tunnel experiments are compared with the theoretical parameters, predicted by extending the Theodorsen theory to a thin airfoil with leading and trailing edges. The effective frequencies measured during the tests follow the theoretical trend. The damping values did not fit so well with the theoretical values, but similar trends were also obtained.

Acknowledgements

This research was supported by the Instituto de Cooperação Científica e Tecnológica Internacional and by the Danish Technical Research Council.

References

[1] HANSEN, H.; THOFT-CHRISTENSEN. P. *Active control of long bridges using flaps.* Proc. of Second World Conf. on Structural Control, Kyoto, 1998.

[2] KWON, S; CHANG, S.; KIM, Y. *Active suppression of flutter and gust response of bridges using edge control surfaces.* Proc. of 10th Int. Conf. on Wind Engineering, Copenhagen, 1999, pp. 941-946.

[3] HANSEN, H. *Active vibration control of long suspension bridges*, Ph.D. Thesis, Aalborg University, 1998.

[4] OSTENFELD, K.; LARSEN, A. *Elements of active flutter control of bridges.* Proc. of New Technologies in Structural Engineering, LNEC, Lisbon, 1997, pp. 683-694.

[5] *European Patent Specification. A system and a method of counteracting wind induced oscillations in a bridge girder*. EP 0 627 031 B1. Bulletin 1996/24.

[6] SIMIU, E.; SCANLAN, R. *Wind effects on structures. Fundamentals and applications to design*, John Wiley & Sons, 3rd edition, New York, 1996.

STRUCTURAL RELIABILITY THEORY SERIES

PAPER NO. 183: P. Thoft-Christensen: *Assessment of the Reliability Profiles for Concrete Bridges*. ISSN 1395-7953 R9823.

PAPER NO. 184: H. I. Hansen, P. Thoft-Christensen: *Active Control of Long Bridges using Flaps.* ISSN 1395-7953 R9838.

PAPER NO. 185: H. I. Hansen, P. Thoft-Christensen: *Wind Tunnel Experiments with Active Control of Bridge Section Model.* ISSN 1395-7953 R9839.

PAPER NO. 186: H. I. Hansen: *Active Vibration Control of Long Suspension Bridges*. Ph.D. Thesis. ISSN 1395-7953 R9840.

PAPER NO. 187: P. Thoft-Christensen: *Estimation of the Service Lifetime of Concrete Bridges*. ISSN 1395-7953 R9851.

PAPER NO. 188: P. Thoft-Christensen: *Future Trends in Reliability-Based Bridge Management.* ISSN 1395-7953 R9936.

PAPER NO. 189: D.M. Frangopol, P. Thoft-Christensen, P.C. Das, J. Wallbank, M.B. Roberts: *Optimum Maintenance Strategies for Highway Bridges.* ISSN 1395-7953 R9937.

PAPER NO. 190: P. Thoft-Christensen: *Estimation of Bridge Reliability Distributions.* ISSN 1395-7953 R9938.

PAPER NO. 191: P. Thoft-Christensen: *Stochastic Modelling of the Crack Initiation Time for Reinforced Concrete Structures.* ISSN 1395-7953 R0012.

PAPER NO. 192: T. Huynh, P. Thoft-Christensen: *Suspension Bridge Flutter for Girder with Separated Control Flaps*. ISSN 1395-7953 R0013.

PAPER NO. 193: T. Huynh, P. Thoft-Christensen: *Buffeting Response of Suspension Bridge Girder with Separate Control Flaps*. ISSN 1395-7953 R0014.

PAPER NO. 194: T. Huynh: *Suspension Bridge Aerodynamics and Active Vibration Control.* Ph.D. Thesis. ISSN 1395-7953 R0015.

PAPER NO. 195: P. Thoft-Christensen: *Inspection Based Evaluation of a Danish Road Bridge*. ISSN 1395-7953 R9927.

PAPER NO. 196: P. Thoft-Christensen: *On Reliability Based Optimal Design of Concrete Bridges.* ISSN 1395-7953 R0017.

PAPER NO. 197: P. Thoft-Christensen: *Active Control of Suspension Bridges.* ISSN 1395-7953 R0018.

PAPER NO. 198: H.I. Hansen, P. Thoft-Christensen, P.A. Mendes, F.A. Branco: *Wind Tunnel Tests of a Bridge Model with Active Vibration Control.* ISSN 1395-7953 R0019.

PAPER NO. 199: P. Thoft-Christensen: *Modelling of the Deterioration of Reinforced Concrete Structures*. ISSN 1395-7953 R0020.

PAPER NO. 200: A.S. Nowak, P. Thoft-Christensen: *International Contribution to the Highways Agency's Bridge Related Research.* ISSN 1395-7953 R0028.

ISSN 1395-7953 R0019
Dept. of Building Technology and Structural Engineering
Aalborg University, December 2000
Sohngaardsholmsvej 57, DK-9000 Aalborg, Denmark
Phone: +45 9635 8080 Fax: +45 9814 8243
www.civil.auc.dk/i6